Towards a Magnetostrictive Micro-Loudspeaker

Albach, Thorsten [1,2]; Horn, Peter [1]; Ilg, Jürgen[1]; Friedrich, Stefan[1]; Sutor, Alexander[1]; Lerch, Reinhard[1]
[1] Chair of Sensor Technology, University Erlangen-Nuremberg, Paul-Gordan-Str. 3-5, 91052 Erlangen
[2] talbach@lse.eei.uni-erlangen.de

In this contribution, we present the design, performance and calculation model of a micro-actuator (MEMS) which works as a micro-loudspeaker. The device is based on the magnetostrictive effect and basically consists of a comb structure of monomorph bending cantilevers with an active area up to $3.0 \times 2.5\,\mathrm{mm}^2$. It produces a sound-pressure-level up to 101 dB at 400 Hz in a standard 2 ccm measurement volume. We present a mechanic-acoustic-coupled lumped element model to calculate sound pressure. The model incorporates finite element results for mechanical behavior. Measurement results validate our model assumptions. Parameter variations show possible improvements of our prototype actuator design.

1 Introduction

Silicon microphones have created a huge impact on the MEMS market, which leads analysts to predict a promising market share also for MEMS-loudspeakers [1, 2]. But until now, there does not exist any commercial integrated MEMS-device for sound generation in the audio range. However, some effort has been made using electromagnetic, electrodynamic or piezoelectric actuation principles [3, 4, 5, 6].

Here we propose an alternative design for a micro-loudspeaker, based on the magnetostrictive effect [7, 8, 9, 10]. We demonstrate its performance in generating sound pressure in a standard 2 ccm measurement volume. The main advantages of magnetostriction compared to other actuation principles are the high energy density, short reaction times and contactless operation as well as the possibility of low driving voltages due to low actuator impedances [11, 12, 13, 14].

In this paper we will first give a brief introduction to the magnetostrictive effect. Then we introduce our MEMS-device and its fabrication process and show its functionality as a micro-loudspeaker. We introduce a lumped element model of the coupled mechanical-acoustical system and show measurement as well as calculation results. Variations of different parameters show possible improvements of the design. We conclude with an outlook on the next developement steps.

2 Joule Magnetostriction

Magnetostrictive strain as a function of magnetic field strength is a highly nonlinear quantity. At higher fields, the strain is subject to saturation. Magnetostrictive materials also show hysteresis behavoir. Models have been developed to describe these phenomena using e.g. the Preisach hysteresis operator [15].

For many applications, including the one at hand, it is however sufficient to regard linear magnetostriction

$$\lambda = \Delta L / L_0 \tag{1}$$

that results from applying a longitudinal magnetic field on a sample of length L_0 which thus changes its length by ΔL. λ denotes the magnetostrictive strain. A linear working point needs to be set up by applying a DC magnetic field. λ is assumed to be constant around the working point.

More extensive treatment of magnetostrictive effects can be found in literature [11, 12, 13, 14].

3 Design and Fabrication Process

In this section we summarize the setup and fabrication process of our MEMS-device.
It consists of a comb structure of long and narrow monomorph bending cantilevers on a silicon substrate as depicted in Fig. 1. There are two rows of cantilevers opposite to each other. Each cantilever consists of one active, magnetostrictive layer and at

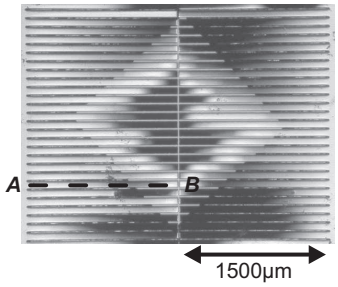

Figure 1: Microscope photography of MEMS-device.

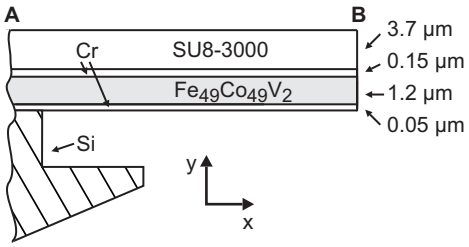

Figure 2: Cross section of one bending cantilever.

least one passive layer. Fig. 2 shows the cross section, including layer thicknesses, along the line *A-B* as indicated in Fig. 1. If an external magnetic field is applied parallel to the cantilevers, the lower, magnetostrictive layer elongates and the cantilevers bend upwards.

We use Vanadium Permendur ($Fe_{49}Co_{49}V_2$) as magnetostrictive material and the epoxy-based negative photoresist SU8-3000 (MicroChem Corp., Newton, MA, USA) as main passive layer. Chromium (Cr) is used as adhesion layer. The layers are applied using HF-magnetron sputtering and spin coating process. The cantilevers are freed from the substrate in the last processing step using anisotropic silicon etching in KOH. Below the cantilevers, a hole is etched to the backside of the substrate at an angle of 45° (Fig. 1) to ensure a certain backvolume for sound generation. Cantilever width is always 75 µm and mutual distance amounts to 10 µm.

We fabricate the device in different sizes. Here, we show cantilever lengths of 1000 µm with a total number of 40 cantilevers each and lengths of 1250 µm and 1500 µm with a total number of 58 cantilevers each. The corresponding active areas are 2010x1710 μm^2, 2510x2475 μm^2 and 3010x2475 μm^2. Variations of the design and the fabrication process have been discussed in detail [7, 8, 9].

4 Micro-Loudspeaker

The given magnetostrictive MEMS-device is actuated by an external AC magnetic field of the desired audio frequency. The field is aligned parallel to the cantilevers. An additional DC magnetic field shifts the working point to a nearly linear region of the characteristic curve. If we do not shift the working point away from zero, frequency doubling occurs due to the nearly quadratic nature of the magnetostrictive effect. Both magnetic fields are currently generated by a turning magnet wheel and a field coil respectively [16]. In a next step, these field generators will be miniaturized to be included into a single micro-loudspeaker chip [10].

Sound pressure is measured inside a 2 ccm standard measurement volume which is connected to the micro-actuator via a small rubber tube. The tube is pressed on top of the micro-actuator and has a diameter of 5 mm over a length of 1.5 mm and then changes its diameter to 1 mm over a length of 5 mm before entering the measurement volume [16].

5 Model Setup

In order to understand and optimize the micro-actuator and its performance as a micro-loudspeaker we present a calculation model for the coupled system.

Acoustical Network

Since the physical dimensions of our micro-loudspeaker are small compared to audio wavelengths in air, it is possible to model the acoustic network using lumped elements [17, 18]. We make use of the electroacoustical analogy which maps the acoustic pressure p to the electric voltage U and the volume flux q to the electric current I. The resulting acoustic lumped element model is depicted in Fig. 3. We are interested in the sound pressure p_0 in the measurement volume which is modeled as an acoustic compliance N_0. The narrow section of the rubber tube is represented by a mass and a friction element M_t, R_t, whereas the wide section of the tube resembles another compliance N_1. The air-gaps between the cantilevers are modeled with a friction element R_a. The corresponding equations are [17, 18]

$$N_{0;\,1;\,2} = \frac{V_{0;\,1;\,2}}{\rho\, c^2} \quad , \qquad R_a = \frac{12\,\eta\, t_c}{w_a^2\, A_a} \quad ,$$
$$M_t = \frac{\rho\,(l_t + r_t\,\pi/2)}{\pi\, r_t^2} \quad , \quad R_t = \frac{8\,\eta\, l_t}{\pi\, r_t^4} \quad , \quad (2)$$

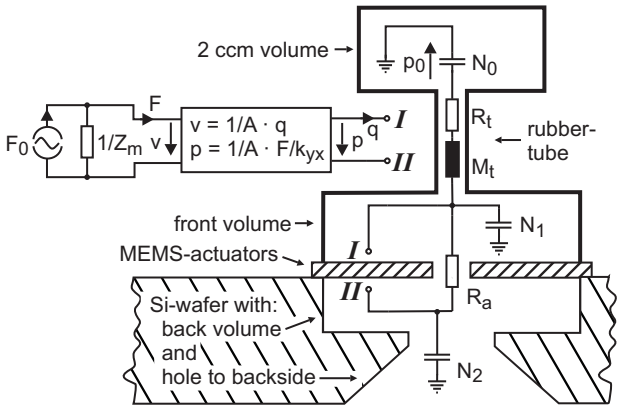

Figure 3: Lumped element model.

where $V_{0;1;2}$ are the volumes of the corresponding cavities, $c = 343\,\mathrm{m/s}$ is the sound velocity, $\rho = 1.2\,\mathrm{kg/m^3}$ is the air density, $\eta = 1.8 \cdot 10^{-5}$ kg/m/s is the viscosity of air, l_t is the length of the narrow section of the tube, r_t is its radius, t_c is the thickness of one cantilever, w_a is the width of the airgap between two cantilevers and A_a is the total area of the airgaps between the cantilevers.

Mechanical Network

The moving cantilevers act as an acoustic source at connectors I and II. To describe this source, we additionally model the mechanical behavior of the microactuators and use the electromechanical analogy. Velocity v corresponds to voltage U and force F corresponds to current I. We apply a sinusoidal force source F_0, which results from magnetostriction, and describe the cantilevers mechanical behavior by their admittance $1/Z_m$ (Fig. 3), since the chosen analogy behaves reciprocal concerning impedances [17, 18].

The amplitude of the driving force F_0 is approximated by applying Hooke's Law to the magnetostrictively strained cantilever layer (see eq.1)

$$F_0 = \lambda\, E_{c1}\, A_{c1} \;=\; \lambda\, E_{c1}\, t_{c1}\, w_c\, n \quad , \qquad (3)$$

where A_{c1} is the total cross-section of the active cantilever layer with its thickness t_{c1}, the cantilever width w_c and the total amount of cantilevers n in one actuator device. E_{c1} denotes the Young modulus of the magnetostrictive material. The amplitude of the strain λ in the linear working point has to be derived from the magnetostrictive characteristic curve of the active material and has a maximum value of half of the saturation magnetostriction. The mechanical impedance Z_m of the cantilevers is derived from a finite element simulation applying the plain strain formulation (2D). We use the finite element computation kernel CFS++ (Coupled Field Simulation) [19]. In the simulation the cantilever is clamped on one side and a sinusoidal force in x-direction F_x is applied to each node inside the magnetostrictive layer (Fig. 2). As a result, the cantilever moves in y-direction. The impedance as a function of frequency f is then derived from the sum of the applied forces and the average velocity in y-direction as

$$Z_{m,xy}(f) = \frac{\sum F_x(x,y)}{\overline{v_y}(f,x)} \, \frac{w_c\, n}{1\mathrm{m}} \quad . \qquad (4)$$

Our plain strain formulation assumes a width of the cantilever of 1 m. In accordance with the driving force (eq. 3) we have to scale the impedance to the total width $n\, w_c$ of all cantilevers in one actuator device (eq. 4).

Coupled Network

The coupling between the mechanical and the acoustical networks follows the gyrator-type equations depicted in Fig. 3. Before reducing the dimensions of the 2D finite element model and incorporating it into the 1D lumped element model, we have to take care that all physical quantities are defined along the same coordinate axis. This is not the case for the mechanical forces. The magnetostrictive force applied inside the micro-actuator works in x-direction whereas the force which generates the sound pressure (as well as the force wich *results* from the sound pressure) works in y-direction. We therefore calculate a second mechanical impedance $Z_{m,yy}$ from the finite element model, where we apply a force F_y to each node inside the magnetostrictive layer, but in y-direction

$$Z_{m,yy}(f) = \frac{\sum F_y(x,y)}{\overline{v_y}(f,x)} \, \frac{w_c\, n}{1\mathrm{m}} \quad . \qquad (5)$$

$Z_{m,xy}$ and $Z_{m,yy}$ are proportional to each other, as long as excitation frequencies are far below the eigenfrequency for the second eigenmode of the bending cantilever. Now we can adjust the force acting on the micro-actuator in y-direction by a factor

$$k_{yx} = \frac{\overline{Z_{m,xy}}}{\overline{Z_{m,yy}}} \qquad (6)$$

to get the equivalent force in x-direction,

$$F_x = k_{yx} F_y \quad , \qquad (7)$$

which has the same mechanical effect on the microactuator. We use this method to adjust the force direction as seen in Fig. 3. All physical quantities do now act along the same coordinate axis.

From the model (Fig. 3) we can also receive the average velocity of the cantilevers as the voltage v over $1/Z_m$. The average deflection can be derived as $v/(2\,\pi\,f)$ with the frequency f.

6 Results

Measurement data as well as calculation results for the sound pressure level (SPL) in the measurement volume as a function of frequency are presented in Fig. 4. A magnetic flux density of 10 mT amplitude has been applied in a working point of also 10 mT. All measurements have been cunducted in an anechoic measurement room. For further details on the measurements see [16]. Maximum SPL has been measured as 101 dB at 400 Hz with the 1500 µm-device.

In the calculation results in Fig. 4 two cut-off frequencies are clearly distinguishable. The first one at around 450 Hz results from the acoustical resonance of the acoustic network. It can also be observed in the measured data. The second one at higher frequencies results from the mechanical resonance of the cantilevers. With the cantilevers of 1500 µm length, these two frequencies lie close to each other and overlap to one resonance peak. Damping in the mechanic-acoustic system occurs mainly due to the generated sound pressure counteracting the deflection of the cantilevers. The measurement results validate our model.

We can now use the model to vary different parameters of the micro-loudspeaker. At first we change the thickness ratio between the magnetostrictive layer ($Fe_{49}Co_{49}V_2$) and the passive layer (SU8-3000). The overall thickness of the cantilevers is kept contant at 5.1 µm, which is the thickness of the prototype actuator. The adhesion layers are also kept constant in thickness (see Fig. 2). Figure 5 shows the results. We investigate ratios of 1:48 (1 part $Fe_{49}Co_{49}V_2$ to 48 parts SU8-3000) to 21:28. The prototype actuator is produced with a thickness ratio of 12:37. The highest SPL can be achieved with a ratio of 9:40, independent of the length of the actuators.

In a second study we investigate the effect of the width of the airgap w_a between the cantilevers. The airgap is changed between 15 µm and 0.001 µm, where 0.001 µm represents the ideal case of a closed membrane. We employ the optimal layer thickness ratio of 9:40 (see Fig. 5). Total cantilever thickness is as of the prototype actuator. Results are depicted in Fig. 6. The airgap width of the prototype actuator is 10 µm. We can see that, especially for low frequencies, a much better SPL can be achieved with smaller airgaps. The actuator shows nearly closed membrane characteristics with airgaps of 3 µm or smaller.

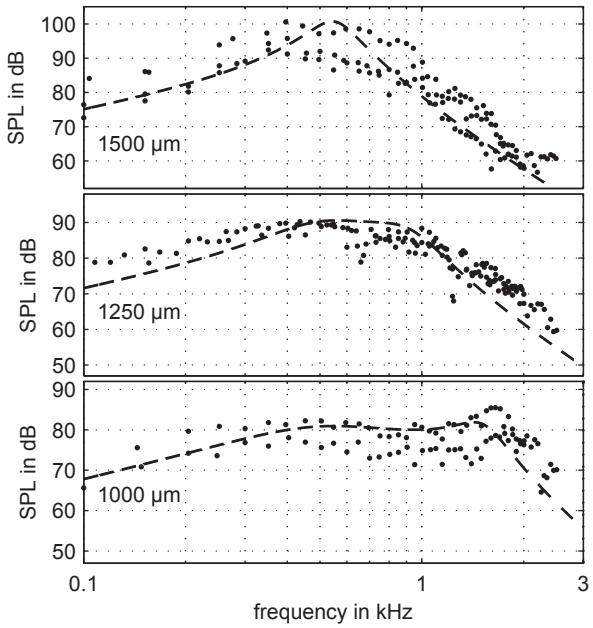

Figure 4: Model results for prototype actuator (dashed line) and measurement data (dots).

7 Conclusion

In this paper we have presented a micro-actuator (MEMS) which is actuated by the magnetostrictive effect and works as a micro-loudspeaker. We introduced the design and fabrication process. A mechanic-acoustic coupled lumped element model has been developed to calculate sound pressure level (SPL) inside a standard 2 ccm measurement volume. The model incorporates finite-element results for the mechanical impedance. Measurement data validates the model. A maximum SPL of 101 dB has been measured at 400 Hz. The calculation model has been used to vary different parameters of the prototype design in order to improve SPL output. In a next step, an improved prototype will be fabricated. Further development will include integrating a field-coil to the micro-loudspeaker to generate the driving magnetic field on-chip.

References

[1] ISuppli, “MEMS Market Tracker - MEMS Back to Double Digit Growth in 2010,” 2010.

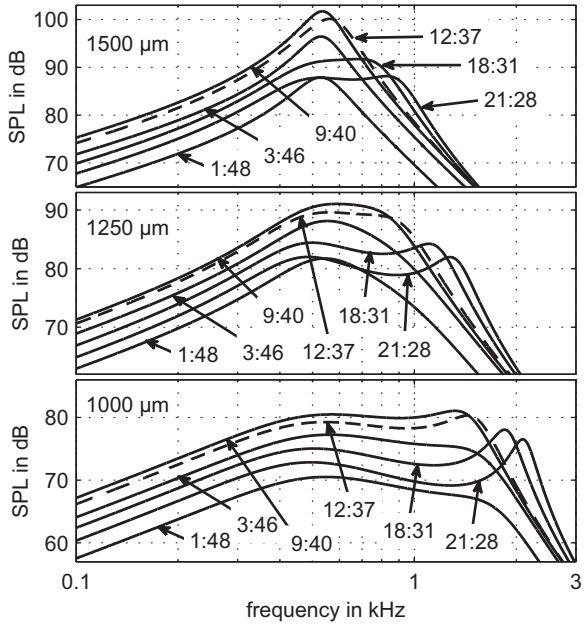

Figure 5: Model results for different layer thickness ratios (active layer : passive layer); total thickness as of prototype actuator; dashed line: prototype actuator

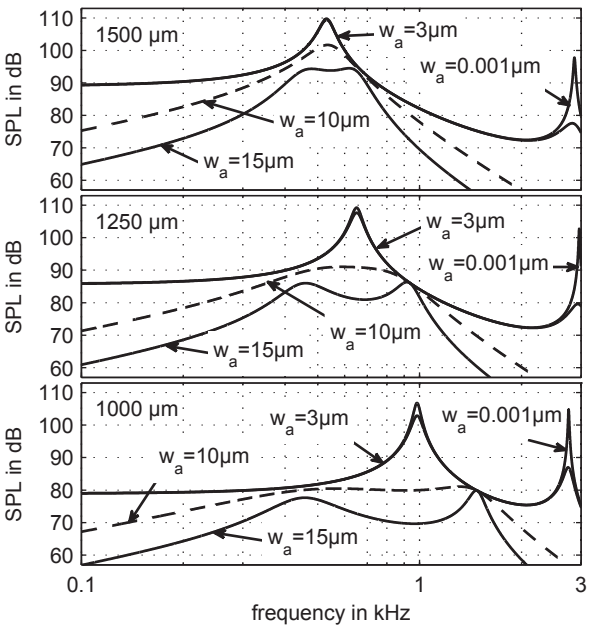

Figure 6: Model results for different airgaps between cantilevers (layer thickness ratio 9:40, see fig. 5); dashed line: airgap of prototype actuator

[2] Yole Developpement, “Emerging MEMS Technologies & Markets - 2010 Report,” 2010.

[3] J. Rehder, P. Rombach, and O. Hansen, “Balanced membrane micromachined loudspeaker for hearing instrument application,” *Journal of Micromechanics and Microengineering*, vol. 11, p. 334, 2001.

[4] M.-C. Cheng, W.-S. Huang, and S. R.-S. Huang, “A silicon microspeaker for hearing instruments,” *Journal of Micromechanics and Microengineering*, vol. 14, pp. 859–866, July 2004.

[5] S.-S. Je, F. Rivas, R. E. Diaz, J. Kwon, J. Kim, B. Bakkaloglu, S. Kiaei, and J. Chae, “A Compact and Low-Cost MEMS Loudspeaker for Digital Hearing Aids,” *IEEE Transactions on Biomedical Circuits and Systems*, vol. 3, pp. 348–358, Oct. 2009.

[6] S. Ko, Y. Kim, S. Lee, S. Choi, and S. Kim, “Micromachined piezoelectric membrane acoustic device,” *Sensors and Actuators A: Physical*, vol. 103, pp. 130–134, Jan. 2003.

[7] T. Albach, B. Baffoun, A. Sutor, and R. Lerch, “Entwicklung eines magnetostriktiven Mikroaktors,” in *MST 2007, Dresden*, 2007.

[8] T. Albach, A. Sutor, and R. Lerch, “Measuring Technology for a Magnetostrictive Microactuator,” *SENSOR+TEST Conference 2009*, pp. 83–87, 2009.

[9] T. Albach, A. Sutor, and R. Lerch, “Untersuchungen an magnetostriktiven Mikroaktoren (Analysis of Magnetostrictive Microactuators),” *tm - Technisches Messen*, vol. 77, pp. 67–73, Feb. 2010.

[10] T. Albach, A. Sutor, R. Lerch, C. Weistenhöfer, and T. Weidner, “Hearing Device with a Sound Transducer and Method for Producing a Sound Transducer,” *US patent no. US 2010/0296681 A1; European patent no. EP 2 254 353 A2*, 2010.

[11] E. du Trémolet De Lacheisserie, *Magnetostriction - Theory and Applications of Magnetoelasticity*. Boca Raton, FL, USA: CRC Press, 2000.

[12] A. Ludwig and E. Quandt, “Giant magnetostrictive thin films for applications in microelectromechanical systems (invited),” *Journal of Applied Physics*, vol. 87, no. 9, pp. 4691–4695, 2000.

[13] R. C. Wetherhold and H. D. Chopra, “Beam model for calculating magnetostriction strains in thin films and multilayers,” *Applied Physics Letters*, vol. 79, no. 23, p. 3818, 2001.

[14] E. Quandt, B. Gerlach, and K. Seemann, “Preparation and applications of magnetostrictive thin films,” *Journal of Applied Physics*, vol. 76, no. 10, p. 7000, 1994.

[15] A. Sutor, S. J. Rupitsch, and R. Lerch, “A Preisach-based hysteresis model for magnetic and ferroelectric hysteresis,” *Applied Physics A*, vol. 100, pp. 425–430, July 2010.

[16] T. Albach, P. Horn, A. Sutor, and R. Lerch, “Sound Generation Using a Magnetostrictive Micro Actuator,” *J. Appl. Phys.*, vol. in press, 2011.

[17] R. Lerch, G. Sessler, and D. Wolf, *Technische Akustik: Grundlagen und Anwendungen*. Berlin, Heidelberg: Springer Verlag, 2009.

[18] A. Lenk, R. G. Ballas, R. Werthschützky, and G. Pfeifer, *Electromechanical Systems in Microtechnology and Mechatronics*. Berlin: Springer, 2010.

[19] M. Kaltenbacher, *Numerical Simulation of Mechatronic Sensors and Actuators*. Berlin, Heidelberg: Springer Verlag, 2nd ed., 2007.